Virtual Adaptation of Physical Phantoms to Datasets Derived from Clinical Tomographic Examinations

Felix H. Schöfer*a, Karl Schneiderb, Christoph Hoeschena
aGSF – Research Center for Environment and Health, member of the Helmholtz Association,
Ingolstädter Landstraße 1, 85764 Neuherberg, Germany;
bDr. von Haunersches Kinderspital der Universität München;
Lindwurmstrasse 4, 80337 München, Germany

ABSTRACT

Thoracic radiography was simulated making use of a virtual pediatric model created from tomographic data (voxelphantom) of a child eight weeks old. The dataset was scaled down to fit the dimensions of a premature newborn. The simulation allows a quantitative and spatially resolved analysis of the x-ray image generation. The transmission behavior of different anatomical regions present in the voxelphantom was compared to the output of the simulation of a step-like phantom made from aluminum and PMMA. The step like structure of the simulated model can be easily built and statements about its x-ray related behavior can be directly validated by means of experiments. A thin contrast plate was placed on each step to make the determination of dependences e.g. between the applied radiation energy and the contrast to noise ratio possible.

Keywords: digital radiography, optimization, pediatric, voxelphantom

1. INTRODUCTION

The work presented here is part of a project aiming for the optimization of digital thoracic radiography of paediatric patients. Improvements in this field are expected to be of great value due to the low contrast features patients present as well as their higher sensitivity to radiation [1]. The common ways to examine and to optimize diagnostic radiology are on the one hand considerations, calculations and measurements on the basis of physical models, on the other hand clinical studies relying on health personnel and patient data. Clinical studies in general are directly connected to practical experience through their results and are therefore directly applicable. Their main disadvantages are the relatively high expense for their accomplishment as well as difficulties in making generalizations. Physical methods are relatively easy and fast to use. However the application of results derived from phantoms e.g. made from PMMA and alloy or from model calculations needs to be well substantiated. In order to fulfil this task we derive real and virtual physical phantoms for measurements and calculations from tomographic data of real patients. This data is available from tomographic datasets of humans that are in use for the calculation of dosimetric quantities of internal and external exposure [2-6]. The method also allows the adaptation of physical models to specific diagnostic questions for the optimization of the connected examination.

*fx@mytum.de; phone +49 89 3187-3463; www.gsf.de/iss/medphys/eng/

Medical Imaging 2007: Physics of Medical Imaging, edited by Jiang Hsieh, Michael J. Flynn, Proc. of SPIE Vol. 6510, 65104L, (2007) · 1605-7422/07/\$18 · doi: 10.1117/12.709463

Proc. of SPIE Vol. 6510 65104L-1

2. METHODS

2.1 Voxelphantoms

At the GSF there are different three-dimensional virtual human phantoms (voxelphantom) created from tomographic data of humans in use for the calculation of dosimetric quantities of internal and external exposure [2-6]. The voxelphantom in use (Fig. 1) was generated from tomographic data of a baby eight weeks old and 4.2kg heavy. The dataset was resized to fit the physical properties of a premature newborn child, as we expect the greatest benefit from adaptation of exposure parameters to the patient for light and low contrast patients. The voxel dimensions were put to the half of their original value leading to a total body mass of 525g. Scaling down the size of a voxelphantom without changing the anatomy ignores compositional changes which might be necessary for evaluation of dosimetric quantities. In our simulations we concentrate on the thoracic region of the phantom. The voxelphantom is due to its low resolution not suitable for detailed imaging calculations. It makes sense to examine large areas like the lung region or the mediastinum in a larger scale transmission simulation.

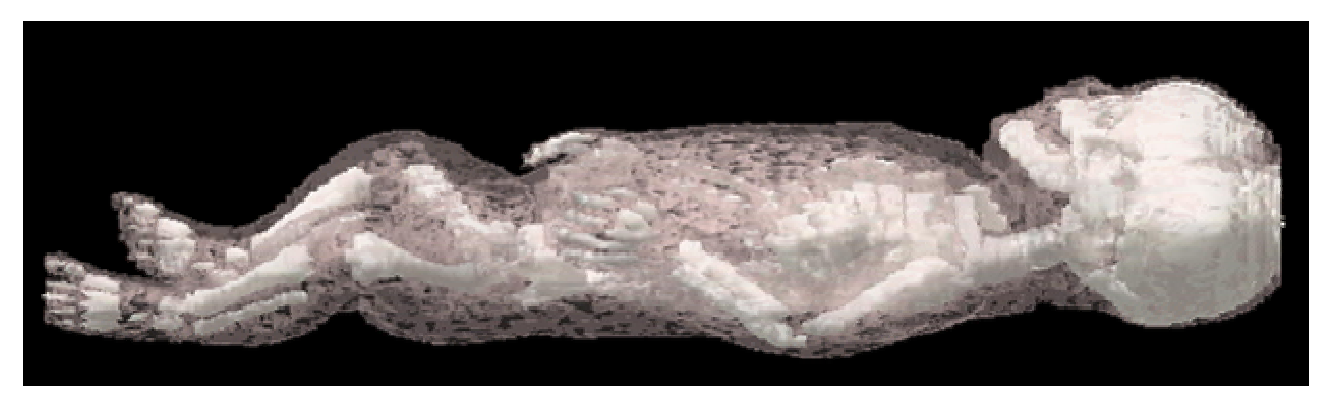


Fig. 1. Representation of skeleton and soft tissue of the voxelphantom in use.

2.2 Step Phantom

The physical phantom used in this project is a modular setup of two crossed step-like structures of PMMA and Alloy. On each step of PMMA an element of 1mm or 1.5mm thickness can be added to provide a low contrast step in the resulting images. The phantom is easy to be built in real (Fig. 2) as well as relatively easy virtually generated in the simulation environment. Fig. 2 shows the real phantom setup which is similar to the virtual phantom we used in the simulations. The steps total thicknesses are 5mm, 6mm, 7mm, and 8mm of aluminum and 20mm 30mm, 40mm, and 50mm of PMMA.

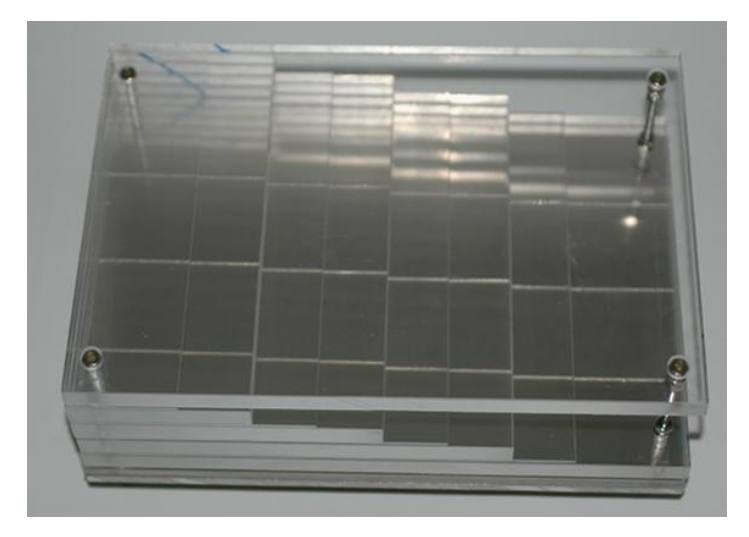


Fig. 2. Modularly built physical phantom of two crossed step-like structures of PMMA and Alloy. Low steps added on the PMMA parts serve as large area contrast elements.

Proc. of SPIE Vol. 6510 65104L-2

Monte Carlo Simulation and Image Evaluation

All Monte Carlo simulations connected to this project were performed using EGS (Electron-Gamma-Shower) in the version EGSnrc. Kawrakow [7] gives a fully self contained description and user manual of EGSnrc. For this project an imaging screen was implemented into the Monte Carlo code in use for dosimetric calculations. The detector plane was programmed to be photon counting. Dependences of detector sensitivity on the energy can be introduced by the simulation of monoenergetic exposure. The detector frame counts photons which have been transmitted through at least one three-dimensional volume element (voxel) of the phantom-region. The simulated imaging resolution is 500*500 pixels. The pixel values are normalised to transmission of the specimen under observation. For this normalisation an empty picture was simulated in the original setting of each phantom. The resulting average input of photons per pixel corresponds to 100% transmission (Fig. 3). Additionally basic information about variation due to the random nature of the simulation is obtained. Between 100 million and 400 million photons were simulated for the imaging. This is a suitable compromise between calculation time and accuracy of the results. The thoracic imaging was simulated with the source located 1m in front of the voxelphantom (AP-projection).

For the evaluation of the transmission behaviour of the simulated specimens we used the IDL software-package for image-analysis [8]. The data derived by those calculations is compared in order to adapt the properties of the physical model to different regions of diagnostic interest of the anthropomorphic model.

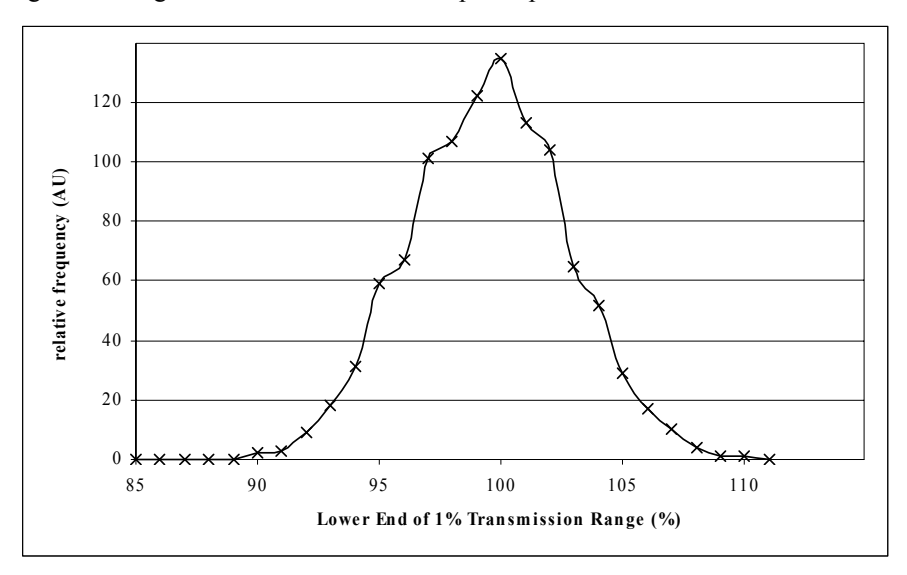


Fig. 3. Transmission Histogram of a background file: The average transmission is 100% as there is no phantom present. The random generation of the sample photons by the Monte Carlo code leads to a spreading around this value. In this case the simulation calculated about 950 input photons per image pixel.

3. RESULTS

3.1 Simulation Results for the Physical Phantom

The crossed steps of differently dense material allow the reproduction and quantification of well known phenomena like e.g. the influence of the tube voltage on the detector noise (Fig. 4, left), and on the contrast produced by a low PMMA step (Fig. 4, right) behind differently thick main absorption. A similar setup is examined theoretically in a connected publication [9]. The total noise rises with the number of photons reaching the detector. The contrast rises with the better penetration through the main absorber and falls with the better penetration through the contrast element. In between there is a maximum. In order to optimize the information gain the contrast has to be put into its relation to the noise.

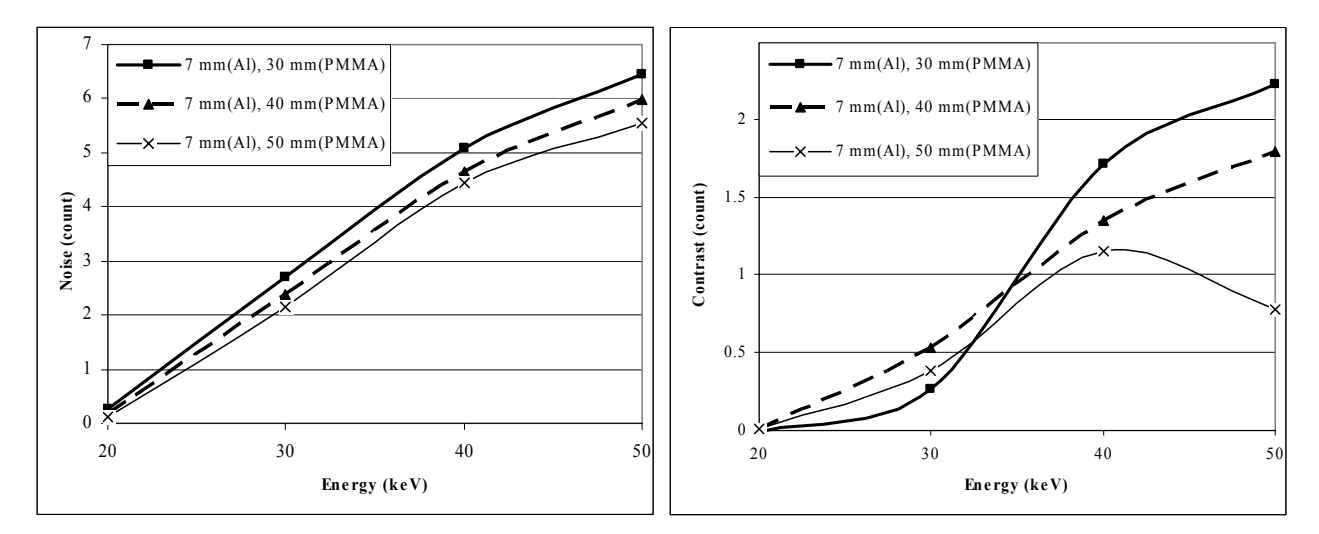


Fig. 4. Noise (left) and Contrast (generated by a 1.5mm PMMA step; right) versus Energy for monoenergetic exposure of different steps of a PMMA and Al step like phantom: The noise rises with the rise of the rising number of transmitted photons at higher energy, the contrast rises to a maximum and falls again.

The signal to noise ratio is rising with the energy of the applied photons (Fig. 5 left). The contrast to noise ratio (Fig. 5 right) delivers the best information about the reproduction of low contrast elements in an image. Its energy dependence is directly connected to the overall thickness of the specimen under observation: For thicker regions it rises with the penetration strength of the applied radiation, for thinner ones it falls with if there is not much change of the absorption attributable to the contrast element, and for regions of medium thickness there are no large effects.

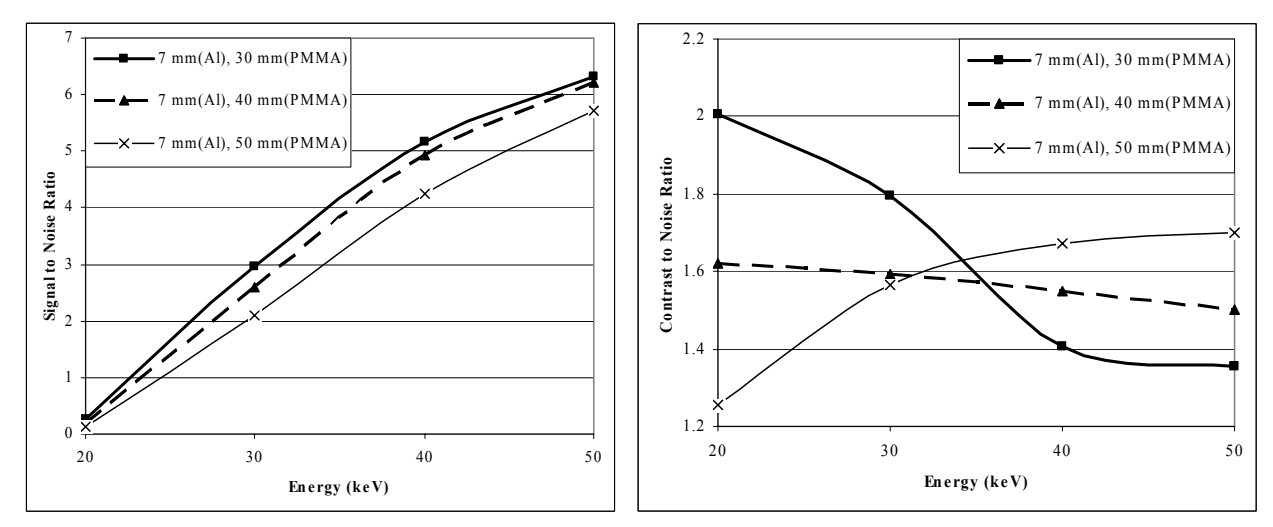


Fig. 5. Signal to noise ratio (left) and Contrast to noise ratio (right) versus Energy for monoenergetic exposure of different steps of a PMMA and Al step like phantom: The signal to noise ratio rises with the penetration strength of the applied radiation but the contrast to noise ratio for the thinnest specimen is best for low and worst at high input energies.

3.2 Simulation Results for the Voxelphantom

The imaging simulation of the voxelphantom delivers information about the lateral distribution of transmission properties of the voxelphantom in use. The simulation was performed for monoenergetic x-ray radiation and different standard x-ray tube spectra. For low energies the specimen absorbs all radiation, for high energies the differences in

absorption by different material or different thicknesses even out. The optimal energy in terms of image generation is a compromise between high enough contrast and high enough penetration of a specimen (Fig. 6).

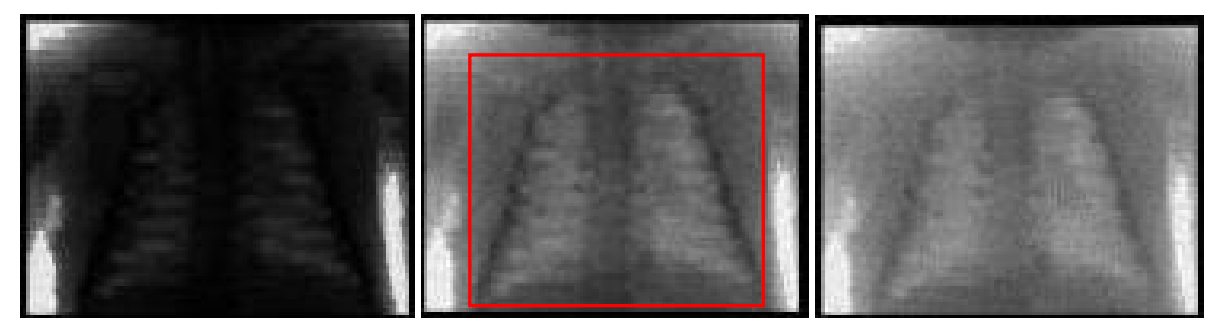


Fig. 6. Simulation of 20keV, 35keV and 50keV (from left to right) monoenergetic thoracic imaging of a 525g baby shown at the same window levels. The red frame in the middle indicates the "whole thorax" region evaluated in the histogram analysis (see text).

The behavior of the thoracic region (marked in Fig. 6) is further analyzed via the frequency of pixels corresponding to a certain transmission in the imaging process (Fig. 7): The range of transmission values found in the image widens and is shifted to higher values with higher applied energy. The transmission appearing most frequently is assigned to most pixels in the image. The connected global maximum in each histogram represents the transmission value for regions of the most common attenuation. Additionally there are pixels imaging the attenuation of other regions like the lung region and the bones introducing local maxima. In the histograms corresponding peaks should appear at values to the left and right of the main transmission. This way it is seen that there is no good discrimination possible between regions more dense with low energies. In a first approach the best visualization of different regions is connected with separated peaks in the transmission histograms. As a side result the overall rise of transmission with higher energies is reproduced (Fig. 8).

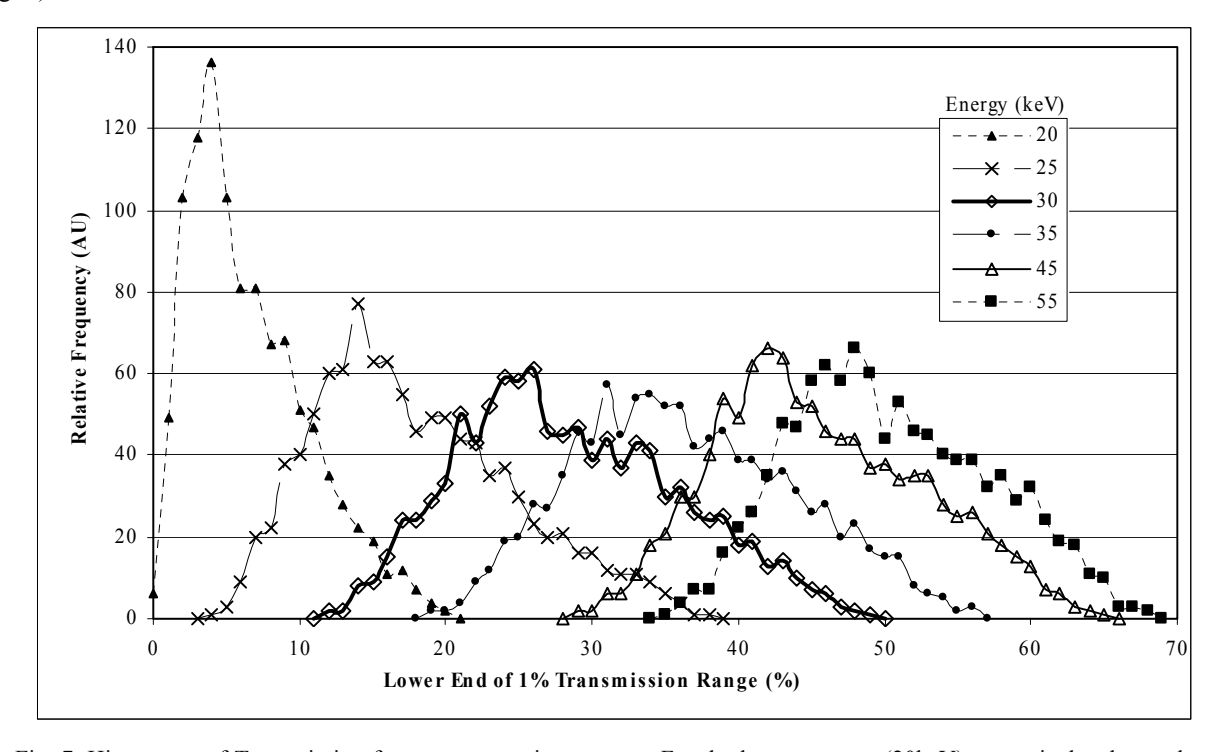


Fig. 7. Histograms of Transmission for monoenergetic exposure: For the lowest energy (20keV) most pixels adopt values corresponding to a single transmission (range between 4% and 5%). For higher energies the histograms show higher transmission values and are widened. The most diversified behavior is found in the medium range of transmission. The area below the histograms is directly proportional to the overall transmission for the thoracic region.

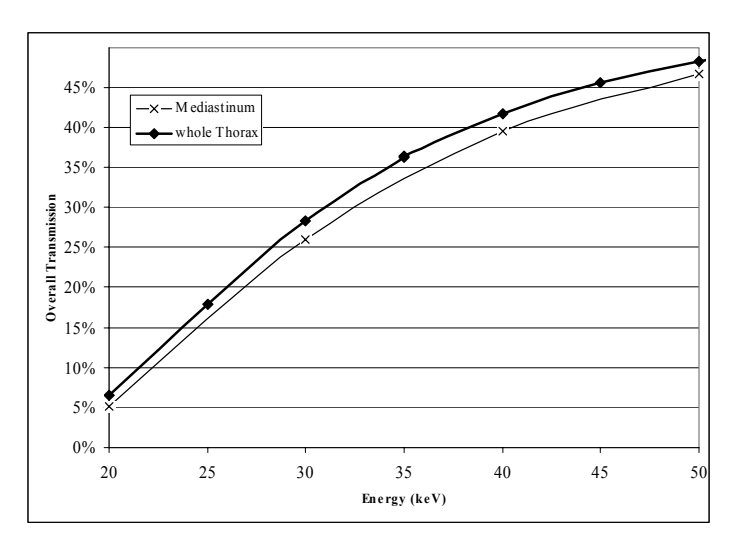


Fig. 8. Share of transmitted photons versus energy of monoenergetic exposure for whole thorax and mediastinum region.

3.3 Adaptation of Voxelphantom and Physical structure

The adaptation of the voxelphantom in the presented context of large area examinations follows via the correlation of the transmission of the regions of interest of the patient to the transmission behavior of different steps of the physical phantom. Figure 9 shows transmission curves for different step thicknesses plotted against the energy of the applied monoenergetic exposure. For low energies the best fit to the behavior of the lightweight newborn by alloy and PMMA would be performed by a 40mm PMMA absorber, for higher energies by 2mm alloy and 10mm PMMA.

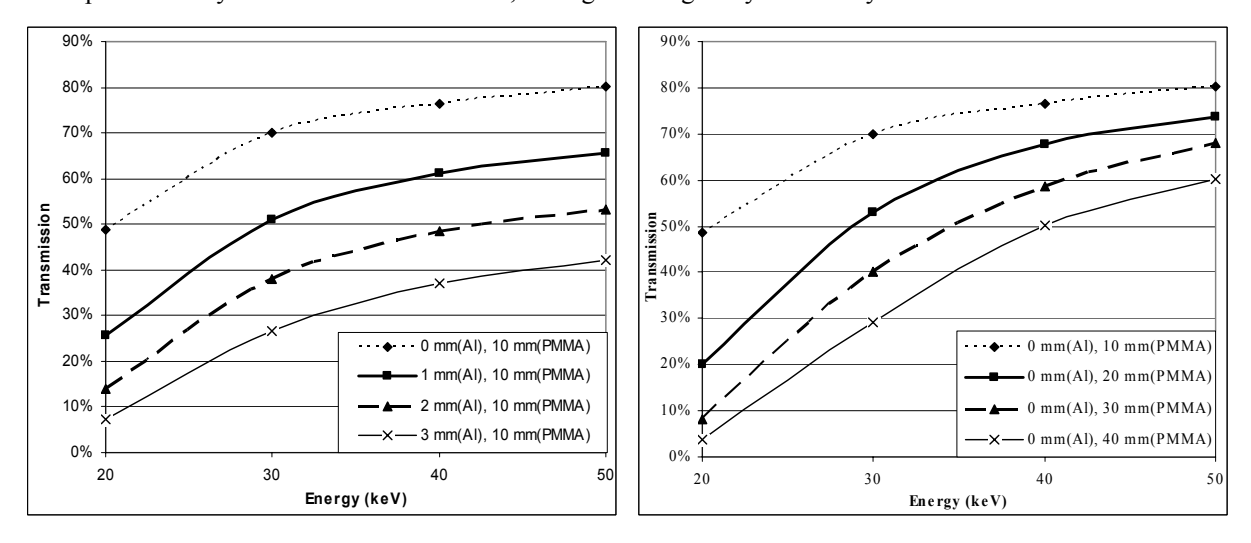


Fig. 9. Share of transmitted photons versus energy of monoenergetic exposure for different steps of a PMMA and aluminium physical phantom.

4. OUTLOOK

As mentioned above the highest effect of optimization of an x-ray imaging process is expected for imaging of thin objects of low overall contrast. In this context a voxelphantom of a premature or newborn child would be highly valuable. The size variation of a model should then lead to recommendations for the exposure in connection with measures like the patients' thickness or weight. Higher resolution voxelphantoms could allow realistic imaging simulations and an exposure adaptation to the region of the actual diagnostic question. In this context different materials

should be evaluated for the use in physical phantoms. The effect of the possible prevention of secondary diagnosis should be examined.

There is no large change in the possible detriment of a low dose exposure over the range of energies of use for clinical relevance to be expected. Nevertheless an assessment of such a change and its inclusion into the evaluation might change the result for an optimal exposure.

5. DISCUSSION

The work presented here shows how the use of voxelphantoms of high resolution can be extended past the calculation of dosimetric quantities. The application in projection radiography is the easiest approach to their application to clinical imaging. With the rise of computational power and improved resolution of the anthropomorphic phantoms the simulation imaging of higher resolution will become possible as well as the simulation of other imaging techniques. The correlation of those simulations to physical models helps to provide clear results of clinical relevance.

6. ACKNOWLEDGEMENTS

We thank M. Zankl and H Schlattl for provision of high quality voxel models and programming experience. The presentation of the results is supported by the Deutsche Forschungsgemeinschaft (German Research Foundation) and the ministry of foreign affairs of the Federal Republic of Germany. The work is part of a project supported by the European research project RISC-RAD under contract number FI 6R-CT2003-508842. The authors thank Prof. Dr. H. Paretzke for supporting this project.

REFERENCES

- United Nations Scientific Committee on the Effects of Atomic Radiation (UNSCEAR), Sources and effects of ionizing radiation, vol. II: Effects. Report to the General Assembly, with annexes. 2000, United Nations: New York
- 2. Zankl, M., et al., *The calculation of dose from external photon exposures using reference human phantoms and Monte Carlo methods. Part VII: Organ doses due to parallel and environmental exposure geometries.* 1997, GSF Forschungszentrum für Umwelt und Gesundheit: Neuherberg, Germany.
- 3. Zankl, M., et al., *The application of voxel phantoms to the internal dosimetry of radionuclides*. Radiation Protection Dosimetry, 2003. **105**(1-4): p. 539-548.
- 4. Zankl, M., et al., *Realistic computerized human phantoms*. Advances in Space Research, 1994. **14**(10): p. (10)423-(10)431.
- 5. Zankl, M., et al., *The construction of computer tomographic phantoms and their application in radiology and radiation protection.* Radiation and Environmental Biophysics, 1988. **27**: p. 153-164.
- 6. Petoussi-Henss, N., et al., *The GSF family of voxel phantoms*. Physics in Medicine and Biology, 2002. **47**: p. 89-106.
- 7. Kawrakow, I. and D.W.O. Rogers, *The EGSnrc code system: Monte Carlo simulation of electron and photon transport*. 2003, National Research Council of Canada (NRCC): Ottawa.
- 8. *IDL.* 2004, Research Systems, Inc.
- 9. Schöfer, F. and C. Hoeschen, *Minimum Dose Calculation for Different Imaging Tasks in Digital Projection Radiography*. Proceedings of SPIE, 2007.

Proc. of SPIE Vol. 6510 65104L-7